Differential Roles of ATM- and Chk2-Mediated Phosphorylations of Hdmx in Response to DNA Damage†

Yaron Pereg,[1] Suzanne Lam,[2] Amina Teunisse,[2] Sharon Biton,[1] Erik Meulmeester,[2] Leonid Mittelman,[3] Giacomo Buscemi,[4] Koji Okamoto,[5] Yoichi Taya,[5] Yosef Shiloh,[1]* and Aart G. Jochemsen[2]*

Department of Molecular Genetics and Biochemistry[1] and Interdepartmental Core Facility,[3] Sackler School of Medicine, Tel Aviv University, Tel Aviv 69978, Israel; Department of Molecular Cell Biology, Leiden University Medical Center, Leiden, The Netherlands[2]; Department of Experimental Oncology, Istituto Nazionale Tumori, Milan 20133, Italy[4]; and Radiobiology Division, National Cancer Center Research Institute, Tokyo 104-0045, Japan[5]

The p53 tumor suppressor plays a major role in maintaining genomic stability. Its activation and stabilization in response to double strand breaks (DSBs) in DNA are regulated primarily by the ATM protein kinase. ATM mediates several posttranslational modifications on p53 itself, as well as phosphorylation of p53's essential inhibitors, Hdm2 and Hdmx. Recently we showed that ATM- and Hdm2-dependent ubiquitination and subsequent degradation of Hdmx following DSB induction are mediated by phosphorylation of Hdmx on S403, S367, and S342, with S403 being targeted directly by ATM. Here we show that S367 phosphorylation is mediated by the Chk2 protein kinase, a downstream kinase of ATM. This phosphorylation, which is important for subsequent Hdmx ubiquitination and degradation, creates a binding site for 14-3-3 proteins which controls nuclear accumulation of Hdmx following DSBs. Phosphorylation of S342 also contributed to optimal 14-3-3 interaction and nuclear accumulation of Hdmx, but phosphorylation of S403 did not. Our data indicate that binding of a 14-3-3 dimer and subsequent nuclear accumulation are essential steps toward degradation of p53's inhibitor, Hdmx, in response to DNA damage. These results demonstrate a sophisticated control by ATM of a target protein, Hdmx, which itself is one of several ATM targets in the ATM-p53 axis of the DNA damage response.

Maintenance of genomic stability is highly dependent on the DNA damage response, an extensive signaling network that is rapidly activated and modulates numerous cellular processes. Genetic defects that disturb this network almost invariably cause severe inherited disorders that are characterized by the degeneration of specific tissues, sensitivity to various DNA-damaging agents, chromosomal instability, and cancer predisposition. Double strand breaks (DSBs), extremely cytotoxic DNA lesions, are very effective in activating the DNA damage response (5). The primary mobilizer of the DSB response in mammalian cells is the nuclear protein kinase ATM, which phosphorylates key players in the various arms of this network (24, 49). One of these players is the p53 tumor suppressor, a sequence-specific transcription factor whose activity is either disabled or attenuated in the vast majority of human cancers (18, 42). Following DNA damage, p53 is stabilized and activated and activates the transcription of many target genes (35). The major biological outcomes are either activation of cell cycle checkpoints (27), which are part of the response leading to cell survival, or induction of apoptosis (51).

In unstressed cells, the half-life and activity of p53 are maintained at low levels to allow normal growth. Regulation of p53 stability and activity is governed by its two negative regulators, Mdm2 and Mdmx (the corresponding human proteins are designated Hdm2 and Hdmx, respectively). Genetic studies suggest that these proteins act as essential, nonredundant negative regulators of p53 during embryonic development (30). Mdm2 interacts with p53, inhibits its activity as a transcription factor, and serves as one of the E3 ubiquitin ligases in p53's proteasome-mediated degradation (39). The gene encoding Mdm2 is transcriptionally activated by p53, creating a negative feedback loop with an important role in the dynamics of p53 levels after stress (37, 39). The Mdmx protein was originally identified as a p53-interacting protein and later as an Mdm2 partner (50, 57). In contrast to Mdm2, Mdmx does not act as an E3 ubiquitin ligase; rather, it interacts directly with p53 and inhibits its transactivation activity (30).

The stabilization and activation of the p53 protein in response to DSBs in DNA is regulated by ATM (35). ATM phosphorylates p53 directly and concomitantly mediates additional phosphorylations and other posttranslational modifications along p53 (35). In addition, ATM targets Hdm2 (22, 34), thereby enhancing its degradation (56). p53's activation also depends on Hdm2-mediated degradation of Hdmx (21, 43). Recently we and others provided evidence that, in response to DSBs, Hdmx is phosphorylated on S403, S367, and S342, of which S403 is a direct ATM target (12, 41, 45). Each of these sites is important for Hdmx-mediated ubiquitination and degradation after DNA damage. We further showed that both ATM's activity and the damage-induced phosphorylations of

Hdmx lead to dissociation of Hdmx and Hdm2 from HAUSP, their deubiquitinase, resulting in destabilization of Hdmx/Hdm2 (36). DNA damage was also reported to promote nuclear accumulation of Hdmx, but the mechanism underlying this phenomenon remained unclear (26). Further experiments established that damage-induced phosphorylation on S367 creates a binding site for several isoforms of the 14-3-3 protein (41). 14-3-3 proteins are a ubiquitous family of molecules that participate in protein kinase signaling pathways within all eukaryotic cells. Functioning as phosphoserine/phosphothreonine-binding modules, 14-3-3 proteins participate in phosphorylation-dependent protein-protein interactions that control, among other processes, the progression through the cell cycle, initiation and maintenance of DNA damage checkpoints, and apoptosis (63).

To better understand the mechanism by which Hdmx phosphorylation in response to DNA damage controls its degradation, we focused on S367 and S342 phosphorylations. While all known DNA damage-induced phosphorylations of Hdmx contribute to its degradation, we find that they do so by different mechanisms. These results demonstrate a sophisticated approach of ATM to a single process, degradation of a target protein, itself just one of several ATM targets in the ATM-p53 axis of the DNA damage response.

(This work was carried out in partial fulfillment of the requirements for the Ph.D. degree of Y. Pereg.).

MATERIALS AND METHODS

Cells. HEK293T, U2-OS, MCF-7, and mouse embryo fibroblast (MEF) cells were grown in Dulbecco's modified Eagle medium with 10% fetal bovine serum and antibiotics.

DNA damaging agents, kinase inhibitors, and LMB. Neocarzinostatin (NCS) was obtained from Kayaku Chemicals (Tokyo, Japan). The ATM inhibitor Ku-55933 was a kind gift from Graeme Smith and Steve Jackson (KuDOS Pharmaceuticals and Wellcome Trust Cancer Research UK and Gurdon Institute, United Kingdom, respectively). The Chk2 inhibitor II was obtained from Calbiochem and leptomycin B (LMB) from Biomol.

Antibodies. Anti-Hdmx antibodies were rabbit polyclonal antibody BL1258 (Bethyl Laboratories, Montgomery, TX), goat polyclonal D19 (Santa Cruz Biotechnology), mouse monoclonal antibodies 6B1A, 11F4D, and 12G11G, and the rabbit polyclonal sera p55, p56, and 1328 (41, 53). The anti-pS367-Hdmx antibody (BL1563) was generated by Bethyl Laboratories. Anti-Mdm2 antibody was mouse monoclonal 4B2 (11), often used in combination with mouse monoclonal SMP14 from Santa Cruz Biotechnology (Santa-Cruz, CA). Anti-ATM antibody was mouse monoclonal MAT3-4G10/8 (3). The anti-p53 monoclonal antibody DO-1, the anti-p53 rabbit polyclonal antibody FL393, and the anti-hemagglutinin (HA) monoclonal antibody F7 were obtained from Santa Cruz Biotechnology. The rabbit polyclonal anti-HA (A190-108A) antibody was produced by Bethyl Laboratories, and the mouse monoclonal anti-LacZ antibody (D19-2F3-2) was obtained from Roche Applied Science (Indianapolis, IN). Anti-pS15-p53, anti-pT68-Chk2, and anti-pT387-Chk2 were obtained from Cell Signaling Technology (Beverly, MA) and the monoclonal antitubulin from Sigma-Aldrich. The rabbit polyclonal anti-HAUSP (BL851) was obtained from Bethyl Laboratories, and the anti-HAUSP monoclonal antibody 1G7 was a gift from Madelon Maurice (36). Anti-pS139-H2AX was the polyclonal antibody BL179 (Bethyl Laboratories) or the monoclonal from Upstate Biotechnology, Inc. (Waltham, MA). Anti-pS957-Smc1 was obtained from Novus Biologicals. The Chk2 monoclonal antibody 44D4 (66) was used for detection by immunoblot analysis, while for immunostaining the polyclonal antibody H300 was used (Santa Cruz Biotechnology). Anti-green fluorescent protein (GFP) rabbit polyclonal antibody was obtained from Novus Biologicals, and the monoclonal anti-GFP was obtained from Roche Applied Science (Indianapolis, IN). Anti-glutathione S-transferase (GST) rabbit polyclonal was obtained from Invitrogen, rabbit polyclonal serum recognizing all 14-3-3 isoforms was obtained from Abcam, and the mouse monoclonal recognizing 14-3-3 tau was obtained from Biosource. Secondary antibod-

ies, horseradish peroxidase-conjugated or fluorescent conjugated, were obtained from Jackson ImmunoResearch.

Immunoblotting analysis and immunoprecipitations. Unless otherwise stated, cell lysates were made in Giordano buffer (50 mM Tris-HCl, pH 7.4, 250 mM NaCl, 0.1% Triton X-100, 5 mM EDTA), supplemented with a mixture of protease and phosphatase inhibitors. Cell lysis, Western blotting analysis, and immunoprecipitations were carried out by standard methods as described previously (14). Immunoprecipitation of endogenous Hdmx to detect S367-phosphorylated Hdmx was performed with a mixture of the monoclonal antibodies 6B1A, 11F4D, and 12G11G (53). To detect endogenous Hdmx/14-3-3 interaction, Hdmx was immunoprecipitated overnight with a mixture of rabbit polyclonal antibodies p56 and 1328 (38). Immunoprecipitation of HAUSP was performed overnight with the BL851 rabbit polyclonal antibody on cell lysates made in Giordano-150 buffer (50 mM Tris-HCl, pH 7.4, 150 mM NaCl, 0.1% Triton X-100, 5 mM EDTA), as has been described before (36). Immunoblots were visualized by enhanced chemiluminescence (Super Signal; Pierce) followed either by autoradiography or detection with the ChemiGenius XE3 system (Syngene, Cambridge, United Kingdom).

Transfection of cell lines. Cells were seeded in Dulbecco's modified Eagle medium for 6 to 24 h and transfected using the FuGENE 6 reagent (Roche Applied Science) according to the manufacturer's instructions.

Expression vectors and in vitro mutagenesis. Expression of recombinant GST-fused Hdmx in *Escherichia coli* was previously described (7). GST-Hdmx was purified from crude *Escherichia coli* lysates with glutathione beads (Amersham Pharmacia). For ectopic expression of Hdmx in human cell lines, the complete open reading frame of the protein was amplified by using the bacterial expression vector as a template, and the product was cloned in the pcDNA3.1 vector (Invitrogen). In vitro mutagenesis of this construct was carried out by the QuikChange in vitro mutagenesis system (Stratagene). The expression vector for Hdm2 was a kind gift of M. Oren (The Weizmann Institute of Science, Rehovot, Israel), and the His₆-ubiquitin plasmid was a gift from David Lane (Dundee, Scotland). The Flag-Chk2 expression vector was described previously (66). The GST 14-3-3 expression vectors were a kind gift of Guri Tzivion (47), the yellow fluorescent protein (YFP)-difopein and YFP-R18(lys) vectors were kindly provided by Haian Fu (31), and the HA-tagged 14-3-3 vector was a gift of Alastair Aitken (13). For stable knockdown in MCF-7 cells, appropriate short hairpin RNA (shRNA) against Chk2 (5′-aaaaaGAGGACTGTCTTATAAAGATTtctct tgaaAATCTTTATAAGACAGTCCTCgggaggatct-3′) or ATM (6) or GFP (5′-gat ccccGGAGCGCACCATCTTCTTCttcaagagaGAAGAAGATGGTGCGCTCCt ttttggaaa-3′) was expressed in the retroviral vector pRetroSuper (9) (a gift from R. Agami). The sequences provided are the primer sequences as cloned into the pRetraSuper vector, with the uppercase letters representing the sequences complementary to the target gene. Cells were infected with retroviral particles according to standard protocols and selected with 5 μg/ml puromycin.

Chk2 kinase assay. The assay was performed as described earlier (32). Briefly, 293T cells were transiently transfected with Flag-Chk2 (1 μg). After 24 h, cells were harvested and lysed, and 1 mg lysate was precleared with 10 μl of Sepharose-protein G at 4°C for 1 h. Lysates were conducted with 10 μl of M2 beads at 4°C for 2 h. Beads were washed twice with lysis buffer and twice with kinase buffer. Kinase reactions were performed by incubating the beads at 30°C for 30 min.

In vivo ubiquitination assay. In all ubiquitination assays, MCF-7 cells were plated into 6-cm dishes 20 to 24 h before transfection. Each dish was transfected with 500 ng of HA-Hdmx, either in the absence or the presence of 200 ng Hdm2, 1 μg of His₆-ubiquitin vector, and where indicated with additional expression vectors. The total amount of DNA always was corrected with the appropriate empty vector. Twenty-four hours after transfection, cells were preincubated with 20 μM MG132 (Calbiochem) for 30 min., after which cells were either mock treated or treated with 500 ng/ml NCS for 5 h, still in the presence of MG132. Cells were then washed twice and scraped in ice-cold phosphate-buffered saline (PBS). Twenty percent of the cell suspension was lysed in Giordano buffer and analyzed by Western blotting. Lysis of the remainder of the cells and the subsequent isolation of His-tagged (ubiquitinated) proteins were performed as described previously (52). Eluates were analyzed by Western blotting.

GST pull-down. To detect GST 14-3-3-interacting proteins in cells, the fusion expression vectors were transfected into U2-OS cells (6 μg/9-cm dish). Twenty-four hours after transfection, cells were preincubated with 20 μM MG132 (Calbiochem) for 30 min, after which cells were either mock treated or treated with 500 ng/ml NCS for 4 h, still in the presence of MG132. Cells were lysed in Giordano buffer, supplemented with protease and phosphatase inhibitors. GST pull-downs were performed for 2 h, tumbling at 4°C, on 750 μg of total protein extract with glutathione beads (Amersham), after which the cells were washed three times in Giordano buffer and bound proteins were eluted by boiling in

Laemmli sample buffer. The eluted proteins were separated by sodium dodecyl sulfate-polyacrylamide gel electrophoresis and subsequently analyzed by Western blotting.

Immunostaining. Cells seeded on glass coverslips were transfected and treated as indicated. After treatment, cells were fixed in 4% paraformaldehyde in PBS for 20 min, followed by a 10-min incubation in PBS containing 0.5% Triton X-100. For staining with the anti-phospho-S367 antibody, coverslips were blocked for 30 min with 1% bovine serum albumin and 10% normal donkey serum in PBS, incubated overnight at 4°C with primary antibodies diluted in primary antibody dilution buffer (Biomeda Corp., Foster City, CA), washed, incubated with secondary antibody for 30 min, and stained with 4′,6′-diamidino-2-phenylindole (DAPI). For the analysis of the Hdmx mutants, coverslips were blocked for 30 to 60 min in PBS–0.05% Tween 20–10% normal goat serum and subsequently incubated with primary antibodies diluted in blocking buffer for 60 to 90 min at room temperature. After three washes with PBS–0.05% Tween 20, coverslips were incubated with secondary antibodies diluted in blocking buffer for 30 min at room temperature. After thorough washing (PBS–0.05% Tween 20), coverslips were mounted in Tris-glycerol buffer containing DAPI. Immunofluorescence analysis was carried out using a Leica TCS SP2 confocal laser scanning microscope or a Leica DM-RXA epifluorescence microscope.

RESULTS

Chk2-mediated phosphorylation of Hdmx on S367 in response to DSBs is essential for Hdmx degradation. Previously we identified DSB-induced phosphorylations of Hdmx on S342, S367, and S403, with S403 being a direct ATM target (45). The sequence surrounding S367 (DCRRTISA) partly overlaps the Chk2 consensus target phosphorylation site (LxRxxS) (55). An in vitro kinase assay showed that Hdmx could be phosphorylated by Chk2. S342A and S367A mutations reduced Chk2-mediated phosphorylation of Hdmx, and a double S342A S367A mutation almost abolished this phosphorylation (Fig. 1A), suggesting that both sites were phosphorylated by Chk2 in vitro. A phospho-specific antibody was successfully raised against the S367 site. This antibody reacted with wild-type but not an S367A mutant Hdmx (Fig. 1B), attesting to its specificity for this site. Hdmx S342A and S403A mutants were phosphorylated on S367 in a manner similar to that of wild-type Hdmx (see Fig. 3B; also data not shown), implying a lack of interdependency of these phosphorylation events. Using this antibody, we monitored S367 phosphorylation of endogenous Hdmx following NCS treatment in stable Chk2- and ATM knockdown derivatives of MCF-7 cells and with the use of specific Chk2 and ATM inhibitors (2, 19) (Fig. 1C and D). The results show that phosphorylation of S367 of Hdmx in response to DSBs is Chk2 and ATM dependent. Collectively, the data suggest that S367 is a direct Chk2 phosphorylation site, and the ATM dependence of this phosphorylation is due to the ATM-dependent activation of Chk2 (1).

Data from our laboratory and other laboratories recently demonstrated that S367 of Hdmx was important for its efficient DNA damage-induced ubiquitination and degradation (12, 41, 45). Accordingly, DNA damage-induced ubiquitination and degradation of Hdmx were found to be Chk2 dependent: knockdown of Chk2 by shRNA or its chemical inhibition strongly inhibited these processes (Fig. 2A to C and 1C and D). Importantly, Chk2 reconstitution in cells knocked down for endogenous Chk2 restored the polyubiquitination pattern of Hdmx following NCS treatment (Fig. 2D). We recently showed that the enhanced polyubiquitination of Hdmx upon DNA damage is, at least partly, due to decreased interaction of Hdmx with the ubiquitin protease HAUSP (36). Indeed, the

dissociation of HAUSP from Hdmx after NCS treatment was attenuated in Chk2-deficient cells (Fig. 2E). These results demonstrate the importance of the ATM-Chk2 axis in damage-induced Hdmx ubiquitination and degradation.

Phosphorylation of S367 and S342 is important for 14-3-3 binding. We recently showed that DNA damage-induced S367 phosphorylation enhances the binding of several isoforms of 14-3-3 proteins to Hdmx (41). In addition, we and others have shown previously that phosphorylation of S342 is also essential for efficient ubiquitination/degradation of Hdmx (12, 45). Interestingly, the sequence surrounding S342 matches a 14-3-3 interaction consensus site "derived from natural interactors which do not exactly match the mode1 and mode2 ligands." These interaction sites are usually rather weak and mainly function in cooperation with a strong interaction site. Furthermore, in such cases dimerization of 14-3-3 is essential for a good interaction (10, 59). To investigate whether dimerization is essential for 14-3-3 binding to Hdmx following DNA damage, we expressed in cells GST-14-3-3 proteins, both the wild type and a dimerization-defective mutant (47). The GST 14-3-3 N-terminal protein cannot interact with its target and is used as a negative control. Interaction between 14-3-3 and Hdmx or p53 was investigated by analyses of bound proteins after pull-down with glutathione beads. Interestingly, wild-type 14-3-3 pulled down Hdmx, and this interaction was enhanced by DNA damage, but the dimerization mutant failed to do so (Fig. 3A). The constitutive binding of 14-3-3 in the untreated cells probably reflects basal phosphorylation of S367, which we previously noticed using the anti-pS367 antibody and also by mass spectrometric analysis (45). p53 is interacting with both the wild type and the dimerization mutant, indicating that the p53 protein has only one 14-3-3 binding site, as was reported (62). We also noticed increased 14-3-3/p53 interaction upon NCS treatment, confirming earlier results (62).

In view of these results, which underscore the importance of 14-3-3 dimer formation in its binding to Hdmx, we explored the relative importance of the different identified phosphorylation sites of Hdmx for 14-3-3 binding. Wild-type and various mutant HA-Hdmx proteins were transiently expressed in cells and used to coimmunoprecipitate endogenous 14-3-3. As expected, mutation of S367 into either alanine or aspartate completely prevented 14-3-3 interaction, while the S403 mutation did not affect the binding between 14-3-3 and Hdmx. Notably, also, the S342A mutant showed reduced interaction with 14-3-3 (Fig. 3B). These results indicate that optimal interaction of 14-3-3 with Hdmx requires dimer formation of 14-3-3 and simultaneous binding to both the S367 and the S342 consensus sites.

All consensus motifs for 14-3-3 binding contain a nonphosphorylated serine or threonine two positions upstream of the phospho-serine/threonine (40). Position 365 in the Hdmx sequence is occupied by threonine. Interestingly, while a T365A mutation did not affect 14-3-3 binding to Hdmx, the corresponding aspartate substitution (T365D) abolished this interaction (Fig. 3B). The Hdmx mutants that still interacted with 14-3-3 (T365A and S403A) showed a basal phosphorylation of S367, which increased following DNA damage. On the other hand, the mutants that completely failed to bind were not detectably phosphorylated (T365D, S367A, and S367D). The S342A mutant behaved exceptionally in that it was still phosphorylated on S367, but its ability to interact with 14-3-3 was
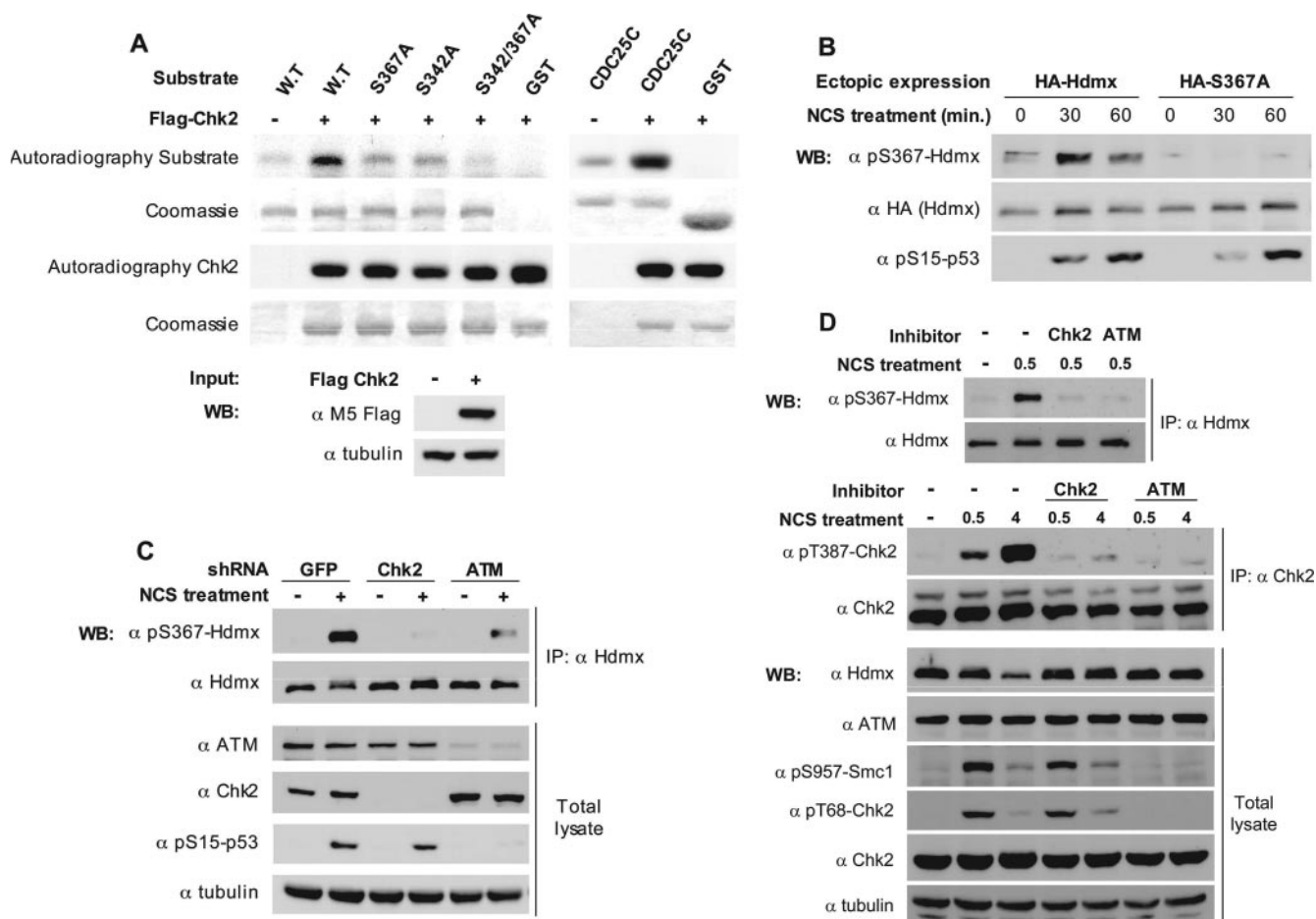
FIG. 1. Chk2 phosphorylates Hdmx in response to DSB. (A) Chk2 phosphorylates Hdmx in vitro. A Chk2 kinase assay was applied to wild-type and mutant versions of recombinant, full-length GST-Hdmx. A GST-Cdc25C fragment (amino acids 200 to 256) containing a Chk2 target, Ser216, was used as a positive-control substrate. The recombinant proteins were incubated with immunoprecipitated wild-type Flag-Chk2. Proteins resolved by sodium dodecyl sulfate-polyacrylamide gel electrophoresis were visualized by autoradiography and Coomassie staining. Note the contribution of both S342 and S367 to the phosphorylation signal. (B) Phosphorylation of Hdmx on S367 in cells in response to DNA damage. HA-tagged Hdmx proteins (1 μg of wild type or S367A mutant) were transfected in U2-OS cells (6-cm dishes). The cells were treated with 200 ng/ml NCS for 30 or 60 min, and cellular extracts were analyzed by immunoblotting with the anti-phospho-S367-Hdmx (α pS367-Hdmx) antibody, anti-HA (α HA) antibody, and the anti-phospho-S15-p53 (α pS15-p53) antibody. The S367 phospho-specific antibody detects the phosphorylation of S367 on wild-type but not on S367A mutant Hdmx. Only phosphorylation of the ectopically expressed protein is detected in this experiment, since the level of endogenous Hdmx is below detection under these conditions. (C) ATM- and Chk2-dependent phosphorylation of endogenous Hdmx on S367. Chk2 or ATM expression was stably knocked down in MCF-7 cells, with GFP-shRNA serving as a negative control. Endogenous Hdmx was immunoprecipitated from lysates of mock-treated and NCS-treated cells (100 ng/ml for 15 min). Immunoblotting analysis of the immunoprecipitates was carried out with the anti-phospho-S367 Hdmx (α pS367-Hdmx) antibody and anti-Hdmx BL1258 (α Hdmx), and the efficiencies of Chk2 and ATM knockdowns were monitored using the corresponding antibodies (α ATM, anti-ATM; α Chk2, anti-Chk2; α pS15-p53, anti-phospho-S15-p53. Antitubulin (α tubulin) was used as a loading control. IP, immunoprecipitation. (D) Effects of Chk2 inhibitor II (2) and the ATM inhibitor Ku-55933 (19) on damage-induced phosphorylation of S367. MCF-7 cells were pretreated with the inhibitors or mock-treated with dimethyl sulfoxide for 30 min and subsequently with NCS (200 ng/ml for 30 min or 4 h). Endogenous Hdmx was immunoprecipitated from the protein lysates and phosphorylation monitored with the anti-phospho-S367 (α pS367) antibody. Endogenous Chk2 was immunoprecipitated from the protein lysates and phosphorylation monitored with the anti-phospho-T387 (α pT387) antibody. Total cellular lysates were also analyzed by immunoblotting with the indicated antibodies. The autophosphorylation of Chk2 on T387 and the appearance of the slower-migrating form of Chk2 served to monitor the activation of Chk2 by ATM and its inhibition by the Chk2 and the ATM inhibitors. Phosphorylation of the cohesin subunit Smc1 on S957 (23, 65) and Chk2 on T68 (33) served to monitor the ATM-mediated DNA damage response and its inhibition by the Ku-55933 inhibitor. Antitubulin (α tubulin) was used as a loading control.

significantly reduced, underscoring the independent importance of this phosphorylation site for the optimal interaction with 14-3-3. These results and those obtained with the 14-3-3 dimerization mutant (Fig. 3A) indicate that, similarly to many other binding partners of 14-3-3 proteins (60), Hdmx binds 14-3-3 via two interaction domains containing phosphorylated serines. The existence of two binding sites for 14-3-3 presents

a molecular basis for preferential binding of a dimeric form of 14-3-3 to Hdmx.

To determine whether indeed Chk2-mediated phosphorylations of Hdmx mediate the increased interaction with 14-3-3, transfections with the GST 14-3-3 expression vector were performed with the Chk2 knockdown and control cells as described for Fig. 3A. Knockdown of Chk2 slightly reduced
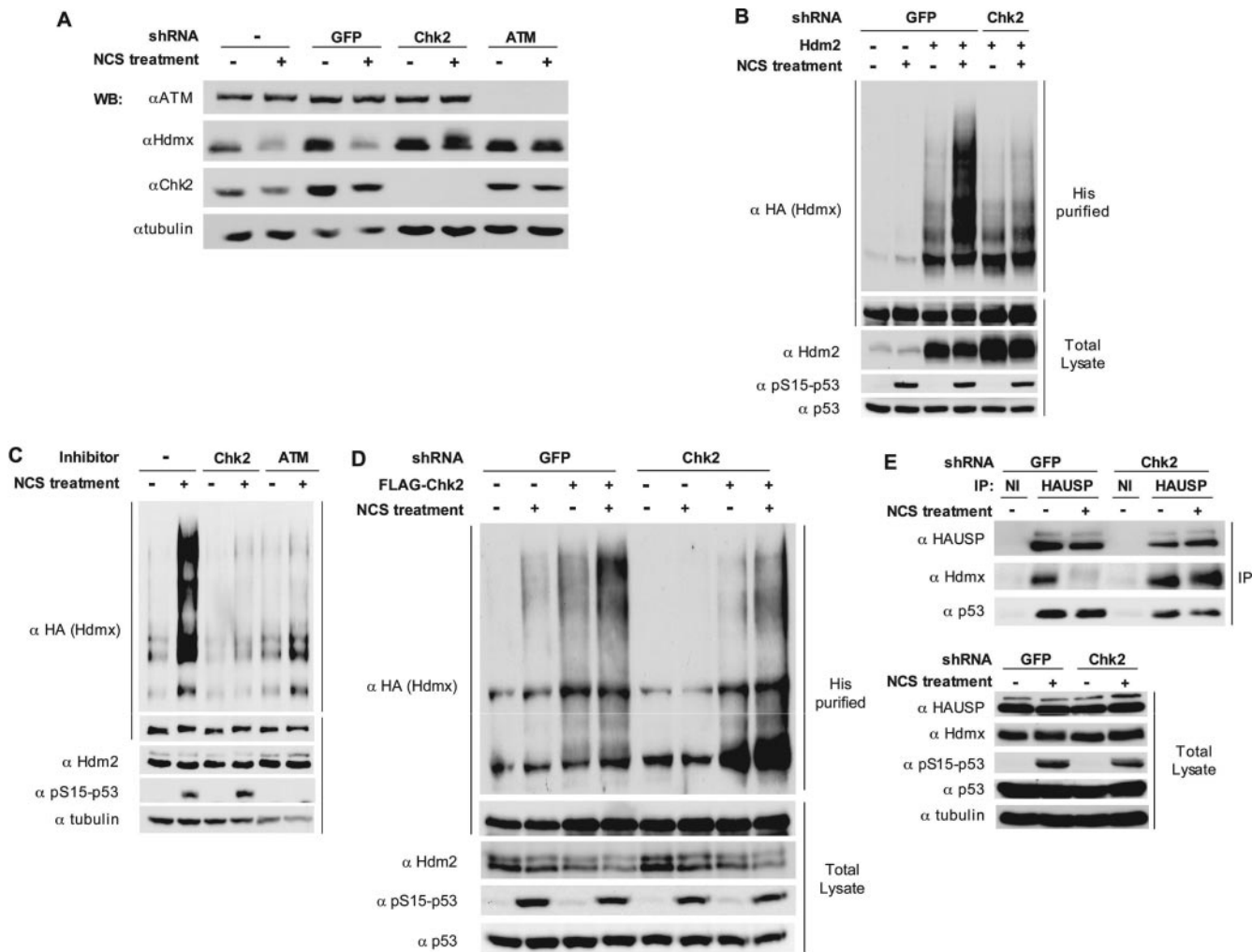
FIG. 2. ATM- and Chk2-dependent degradation and ubiquitination of Hdmx in response to DSBs. (A) Effect of Chk2 and ATM knockdown on damage-induced degradation of Hdmx. The MCF-7-derived cells knocked down for Chk2, ATM, or GFP were treated with 250 ng/ml of NCS for 1 h, and cellular lysates were analyzed by immunoblotting with the indicated antibodies (αATM, anti-ATM; αHdmx, anti-Hdmx; αChk2, anti-Chk2; αtubulin, antitubulin).(B) Effect of Chk2 knockdown on DNA damage-induced ubiquitination of Hdmx. The shGFP- and shChk2-MCF-7 cells were transfected with HA-Hdmx and with His$_6$-ubiquitin expression vectors in the absence or presence of Hdm2. Twenty-four hours after transfection, cells were preincubated with MG132 (20 μM) for 30 min, after which NCS (500 ng/ml) was added. Cells were harvested 5 h later, and analysis of Hdmx ubiquitination and analysis of total extracts were performed as described in Materials and Methods. Antibodies used were anti-HA (α HA) to specifically detect transfected Hdmx, anti-Hdm2 mixture 4B2/SMP14 (α Hdm2), anti-phospho-S15 p53 (α pS15-p53) to monitor DNA damage response, and antitubulin as a loading control. (C) Effect of the Chk2 and ATM inhibitors on damage-induced ubiquitination of Hdmx. HA-Hdmx, Hdm2, and His$_6$-ubiquitin were coexpressed in MCF-7 cells. MG132 (20 μM) and Chk2 inhibitor II (10 μM) or ATM inhibitor Ku-55933 (10 μM) were added 24 h after transfection. Thirty minutes later, 500 ng/ml of NCS was added. Cells were harvested 5 h later, and analysis of Hdmx ubiquitination and analysis of total extracts were performed with the antibodies mentioned in the legend for panel B. (D) Reconstitution of Hdmx ubiquitination by ectopic expression of Chk2 in the Chk2 knocked-down cells. The shGFP- and shChk2-MCF-7 cells were transfected with expression vectors encoding HA-Hdmx, Hdm2, and His$_6$-ubiquitin, either in the absence or presence of the Flag-Chk2 expression vector. Treatment of cells, ubiquitination assay, and immunoblotting were done as described for panel B. It can be seen that the ubiquitination of Hdmx is higher in the control cells (first two lanes) than in the Chk2 knockdown cells (lanes 5 and 6). Coexpression of Chk2 increases the Hdmx ubiquitination in the control cells (lanes 3 and 4) and restores basal and the DNA damage-induced ubiquitination of Hdmx (lanes 7 and 8). (E) Effect of Chk2 knockdown on Hdmx/HAUSP dissociation following DNA damage. The shGFP and shChk2 cells were seeded onto 9-cm dishes. Twenty four hours later, cells were pretreated with MG132 (20 μM) for 30 min, after which some of the dishes were mock treated or treated with 500 ng/ml NCS for 5 h. Subsequently, cells were harvested and the cell extracts used for immunoprecipitations with anti-HAUSP (α HAUSP) or a nonimmune rabbit serum (NI). Immunoprecipitates and total cell extracts were analyzed by immunoblotting analysis. Hdmx was detected with D19 goat polyclonal antibody (α Hdmx), total p53 with DO-1 (α p53), and HAUSP with the IG7 monoclonal antibody. The DNA damage response was monitored with anti-phospho-S15-p53 (α pS15-p53) antibody, and antitubulin (α tubulin) was used as a loading control.

basal interaction between Hdmx and 14-3-3 but strongly inhibited NCS-induced 14-3-3 binding to Hdmx (Fig. 3C). Also, NCS-induced increase of the 14-3-3–p53 interaction, previously shown to be ATM dependent (62), is attenuated

in the Chk2 knockdown cells, which suggests that it is also Chk2 dependent.

Hdmx degradation is stimulated by 14-3-3 binding. The results described above indicate a strong correlation between
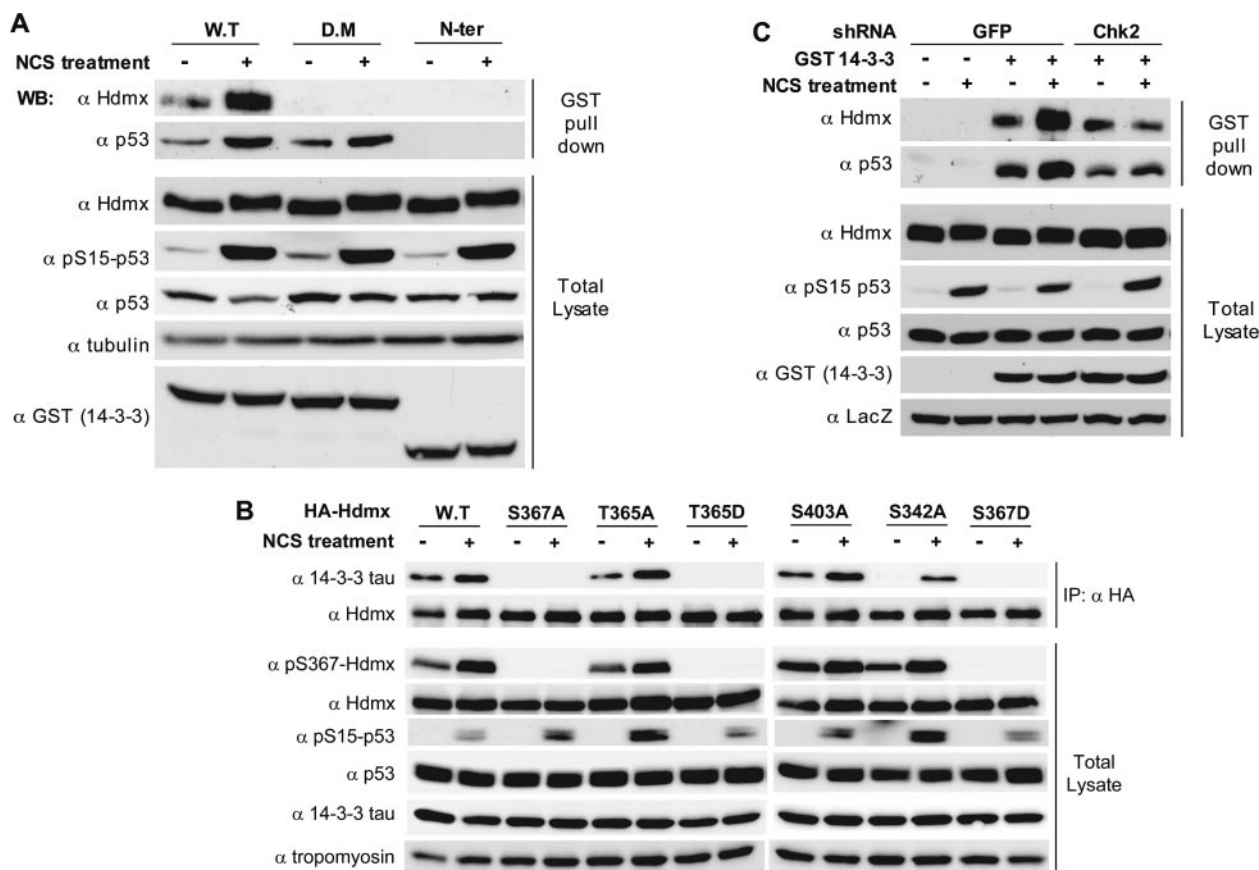
FIG. 3. 14-3-3 proteins bind to phosphorylated Hdmx. (A) Hdmx binding to 14-3-3 is induced in response to DSB and is dependent on 14-3-3 dimerization. U2-OS cells (9-cm dishes) were transfected in duplicate with the GST-14-3-3 wild type (W.T), a GST-14-3-3 dimerization mutant (D.M), and GST-14-3-3 N-terminal (N-Ter) (1–140) constructs. Twenty-four hours later, cells were preincubated with MG132 (20 μM) for 30 min, and subsequently NCS (500 ng/ml) was added for 4 h. Cells were harvested and lysed in Giordano buffer, and the lysates were used for GST pull-down and subsequent immunoblotting analysis. Hdmx was detected with BL1258 (α Hdmx), p53 with DO-1 (α p53), and expression of the GST-14-3-3 constructs with anti-GST (α GST). Anti-phospho-S15-p53 (α pS15-p53) was used to monitor the DNA damage response and antitubulin (α tubulin) as a loading control. (B) Hdmx–14-3-3 interaction is dependent on S367 and S342. MCF-7 cells, 6-cm dishes, were transfected in duplicate with the indicated HA-Hdmx constructs (1 μg/dish). Twenty-four hours later, cells were pretreated with MG132 (20 μM) and subsequently with NCS (500 ng/ml) for 6 h. Cells were harvested and lysed in Giordano (200 mM NaCl) buffer, and lysates were used for immunoprecipitation (IP) overnight with anti-HA (α HA) polyclonal antibody. Immunoprecipitates and total extracts were analyzed by Western blotting (WB) with anti-14-3-3 tau (α 14-3-3 tau), anti-HA to detect Hdmx (α Hdmx), anti-p53 (DO-1) (α p53), and antitubulin. DNA damage response was monitored with anti-phospho-S15-p53. Note that some mutants (S367A, S367D, and T365D), do not detectably coimmunoprecipitate 14-3-3 tau, while the S342A mutant showed reduced efficiency. (C) Increased Hdmx–14-3-3 interaction upon NCS treatment is dependent on Chk2 expression. The shGFP- and shChk2-MCF-7 derivatives, 9-cm dishes, were transfected in duplicate with GST-4-3-3 expression vector. Subsequent analysis was done as described for panel A.

the induced interaction of Hdmx with 14-3-3 after DNA damage and its degradation. However, no causal relationship has yet been demonstrated. To address this point, we decided to make use of a specific peptide, named difopein, that can compete away 14-3-3 from its target proteins, also when expressed as a fusion protein with YFP (25). To investigate whether the YFP-difopein could indeed prevent the Hdmx–14-3-3 interaction, we transfected HA-Hdmx into cells with increasing amounts of YFP-difopein. A mutated version of the peptide, R18(Lys), was used in the highest concentration as a negative control. Hdmx was immunoprecipitated from the cells, and coimmunoprecipitation of 14-3-3 was determined. Indeed, it was found that increasing levels of YFP-difopein diminished the binding of 14-3-3 to Hdmx, while R18(Lys) had only a minor effect (Fig. 4A).

Since the DNA damage-induced phosphorylations and subsequent 14-3-3 interaction correlated with Hdmx degradation, we wondered whether inhibition of Hdmx–14-3-3 interaction could already stabilize Hdmx. Therefore, we followed the expression level of ectopic Hdmx in the presence of various versions of GST-14-3-3 proteins or the YFP-difopein/YFP-R18(Lys) proteins. Coexpression with mutants of 14-3-3 incapable of binding with Hdmx but still containing the dimerization domain, thereby counteracting endogenous 14-3-3 activity by a dominant-negative effect, resulted in higher levels of ectopic Hdmx, while wild-type 14-3-3 did not affect Hdmx levels (Fig. 4B). Similar results were obtained for endogenous Hdmx (Fig. 4C). Similarly, YFP-difopein increased basal levels of HA-Hdmx but not YFP-R18(Lys) (Fig. 4D). Even more important, degrada-
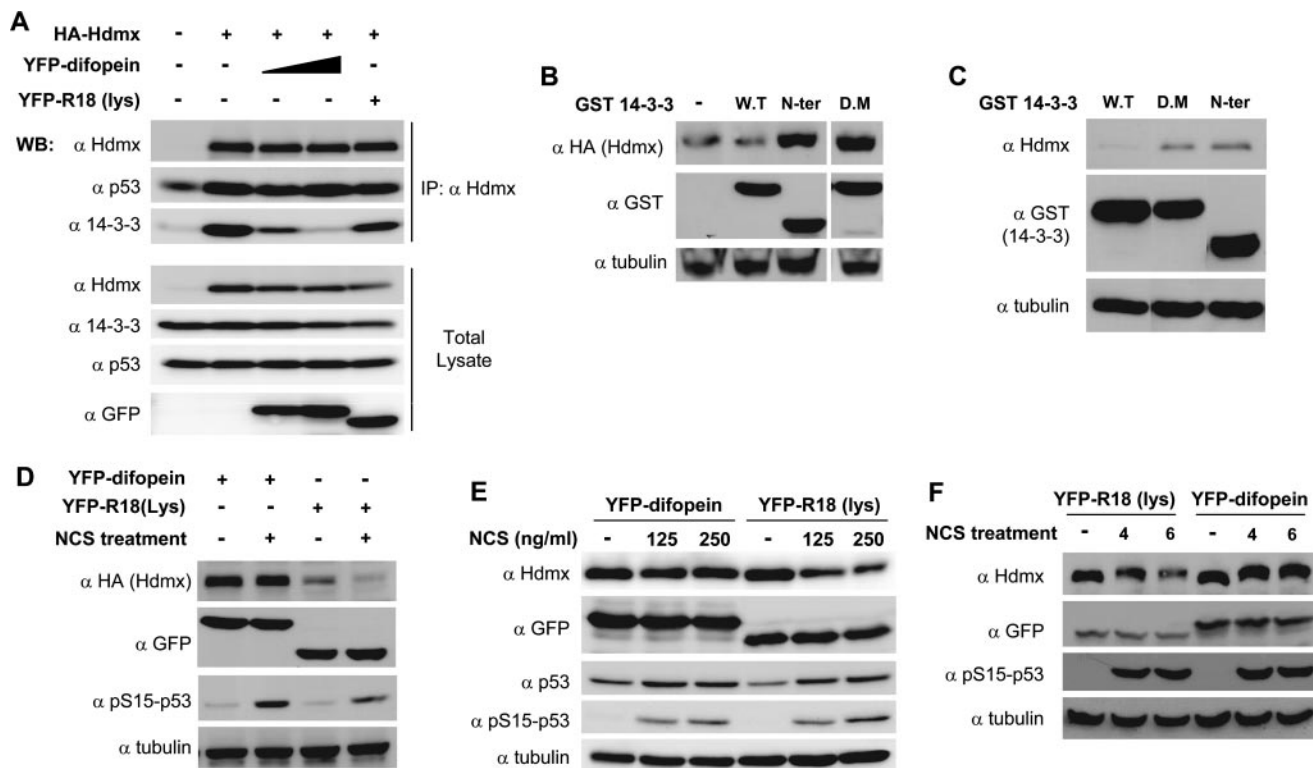
FIG. 4. Interaction with 14-3-3 is needed for efficient Hdmx degradation. (A) YFP-difopein prevents Hdmx–14-3-3 interaction. MCF-7 cells were transfected with HA-Hdmx expression vector in the absence of or with different concentrations of the YFP-difopein vector. YFP-R18(Lys), with a mutated competitor peptide fused to YFP, was used as a control. In all cases the total amount of DNA was adjusted with the appropriate vector. Cells were harvested 24 h after transfection, and cell lysates were immunoprecipitated (IP) with anti-Hdmx (α Hdmx). Both immunoprecipitates and total cell extracts were analyzed by immunoblotting with anti-HA (α Hdmx), anti-p53 (DO-1) (α p53), anti-14-3-3 tau (α 14-3-3), and anti-GFP (α GFP) to monitor the expression of the fusion proteins. YFP-difopein clearly diminishes the amount of 14-3-3 protein coimmunoprecipitated with anti-Hdmx, while YFP-R18(Lys) had no significant effect. (B) Inhibition of 14-3-3 binding increases Hdmx levels. HA-Hdmx (500 ng) and Hdm2 (100 ng) were transiently expressed in MCF-7 cells (6-cm dishes) in combination with various GST 14-3-3 expression vectors (2.5 μg). Forty-eight hours later, cells were harvested and cellular lysates were analyzed by immunoblotting with the indicated antibodies. α tubulin, antitubulin; N-ter, N terminal; D.M, dimerization mutant; W.T, wild type. (C) Inhibition of 14-3-3 binding increases endogenous Hdmx levels. MCF-7 cells (6-cm dishes) were transiently transfected with the various GST 14-3-3 expression vectors (2.5 μg). Forty-eight hours later, cells were harvested and cellular lysates were analyzed by immunoblotting with the indicated antibodies. (D) Effect of inhibition of 14-3-3 on Hdmx degradation in response to DNA damage. HA-Hdmx (500 ng) and Hdm2 (150 ng) were transiently expressed in MCF-7 cells (6-cm dishes) in the presence of the YFP-difopein (2.5 μg) or YFP-R18(Lys) expression vector. Forty-eight hours later, cells were treated with 500 ng/ml NCS and harvested 5 h later. Cellular lysates were analyzed by immunoblotting with the indicated antibodies. (E and F) Effect of inhibition of 14-3-3 binding on endogenous Hdmx degradation in response to DNA damage. U2-OS cells (6-cm dishes) were transfected with either the YFP-difopein or YFP-R18(Lys) expression vector (4 μg/dish). Forty-eight hours later, cells were treated with 125 or 250 ng/ml NCS and harvested 3 h later. Cellular lysates were analyzed by immunoblotting with the indicated antibodies (E). U2-OS cells (10-cm dishes) were transfected with either the YFP-difopein or YFP-R18(Lys) expression vectors (8 μg). Forty-eight hours later, cells were treated with 200 ng/ml NCS and harvested 4 or 6 h later. Cellular lysates were analyzed by immunoblotting with the indicated antibodies (F).

tion of transfected Hdmx (Fig. 4D) and endogenous Hdmx (Fig. 4E and F) after NCS treatment was attenuated in the presence of the YFP-difopein but not with its defective mutant YFP-R18(Lys). Taken together, these results strongly indicate that interaction of 14-3-3 with Hdmx is necessary for efficient degradation of Hdmx.

Phosphorylation of Hdmx on S367 mediates its nuclear retention in response to DNA damage. 14-3-3 proteins are implicated in regulating the subcellular distribution of many phosphorylated target proteins. They are also associated with dynamic nucleocytoplasmic shuttling (28). While in most documented cases they sequester their substrates in the cytoplasm, phosphorylation-dependent binding of 14-3-3 to telomerase was reported to promote its nuclear localization (46), and DNA damage-induced nuclear accumulation of Chk1 in yeast

was shown to be dependent on interaction with Rad24, a 14-3-3 protein (15). Hdmx was reported to translocate into the nucleus following DNA damage (26). Since phosphorylations of S367 and S342 mediate Hdmx binding to 14-3-3, we investigated the importance of these sites for DSB-induced spatial dynamics of Hdmx by following the subcellular distribution of wild-type and mutant Hdmx proteins upon DSB induction. As reported, we found an increased nuclear accumulation of Hdmx upon NCS treatment. Quantification revealed that following treatment for 3 h with 500 ng/ml NCS, over 80% of the transfected cells showed a predominant nuclear localization of Hdmx. Similarly, the S403A and T365A mutants, which could still interact with 14-3-3, accumulated in the nucleus with comparable efficiency (Fig. 5A). Incubation with other DSB-inducing agents, like etoposide, gave similar results (data not
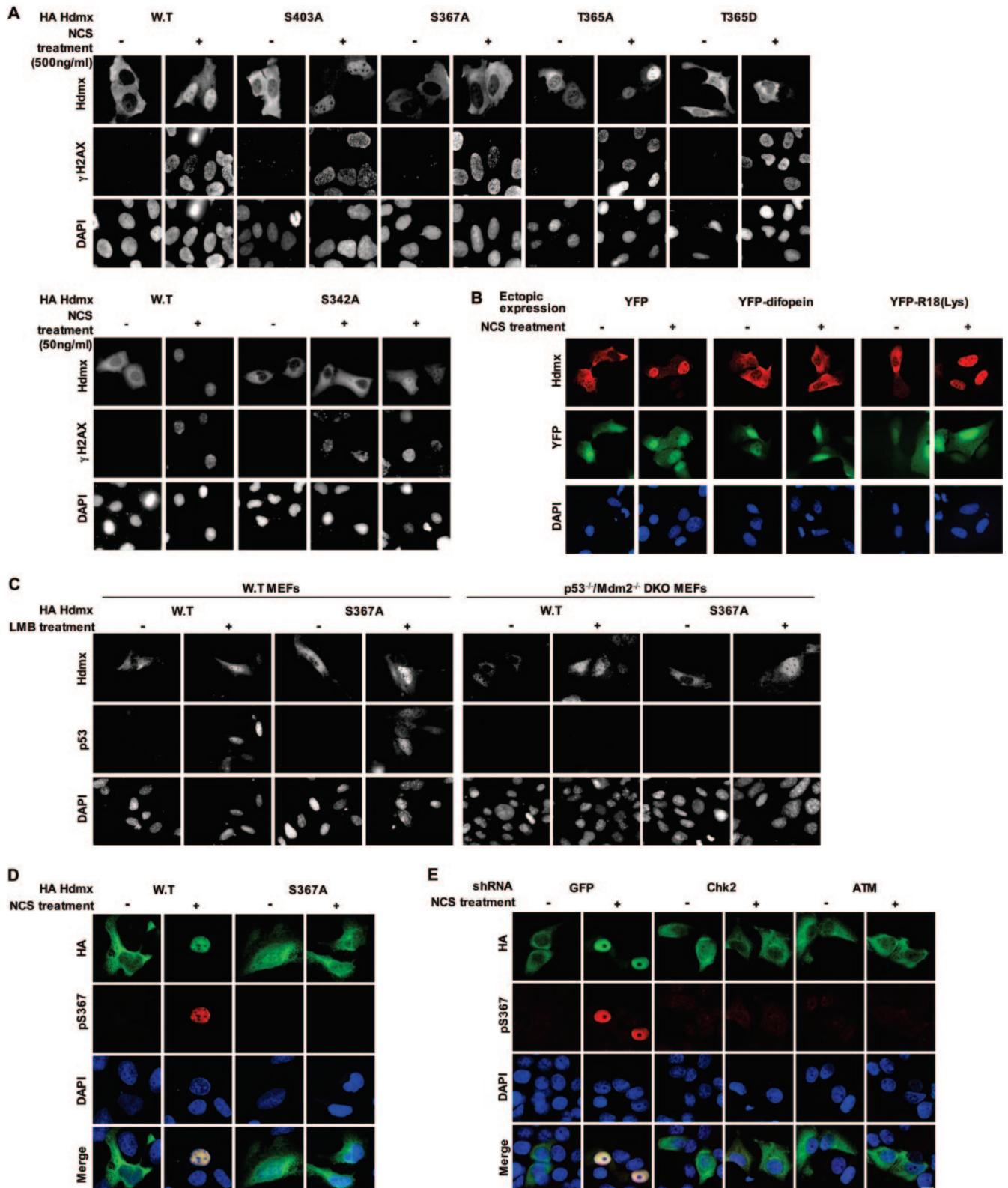
FIG. 5. Phosphorylation of Hdmx is required for its nuclear accumulation. (A) Effect of mutating the Hdmx phosphorylations sites on DSB-induced nuclear accumulation of Hdmx. U2-OS cells were seeded on coverslips in 6-cm dishes 16 to 24 h before transfection. Cells were transfected with 125 ng of HA-Hdmx expression plasmid per dish, with the total amount of DNA adjusted to 2 μg per dish. Twenty-four hours after transfection, cells were treated with NCS, either 500 ng/ml (upper panel) or 50 ng/ml (lower panel) for 3 h. Cells were processed for immunofluorescence and stained with a combination of anti-Hdmx monoclonal antibody (6B1A) and a rabbit polyclonal serum specifically recognizing γ-H2AX to monitor the DNA damage response. Nuclei were stained with DAPI. Pictures were taken with a magnification ×63 lens.

shown). Significantly, substitution of S367 for alanine or aspartate and aspartate substitution of T365 completely abolished nuclear accumulation of Hdmx, again correlating with the loss of 14-3-3 interaction. S342A mutation also reduced this accumulation, albeit to a lesser extent, which was noticed after low doses of the DNA damaging agent (Fig. 5A). Following treatment for 3 h with 50 ng/ml NCS, staining disclosed that only about 25% of the cells in the S342A mutant were predominantly nuclear and 62% were equal nuclear/cytoplasmic, whereas for the wild-type Hdmx, 66% of the cells were mainly nuclear and 25% divided equally between the nucleus and the cytoplasm. Importantly, DSB-induced nuclear accumulation of wild-type Hdmx was inhibited in the cells stably knocked down for Chk2 (see Fig. S1 in the supplemental material). Furthermore, pretreatment of cells with Chk2 and ATM inhibitors also precluded the nuclear accumulation of Hdmx (see Fig. S2 in the supplemental material).

To examine the direct involvement of 14-3-3 interaction in Hdmx accumulation, we prevented the Hdmx–14-3-3 interaction by cotransfection with the YFP-difopein expression vector or with its negative control, YFP-R18(Lys), and nuclear accumulation of wild-type Hdmx was followed after DSB induction. While nuclear accumulation of HA-Hdmx was still observed after coexpression of YFP or the YFP-R18(Lys) protein, coexpression of the YFP-difopein protein inhibited this process (Fig. 5B).

Damage-induced nuclear accumulation of Hdmx could be the result of either increased nuclear import of phosphorylated Hdmx from the cytoplasm or retention of Hdmx molecules that are phosphorylated in the nucleus. Both ATM and Chk2 are primarily nuclear kinases in the absence of and following DSB induction (see Fig. S3 in the supplemental material), as described previously (4, 8), making the second option more likely. To investigate whether Hdmx could enter the nucleus in a DNA damage- and S367-phosphorylation-independent manner, we expressed both wild-type and S367A HA-Hdmx in MCF-7 cells that were subsequently mock treated or treated with LMB, which blocks nuclear export. Intriguingly, both wild-type and S367A HA-Hdmx accumulated in the nucleus upon LMB treatment (see Fig. S4 in the supplemental material). As expected, we observed increased nuclear p53 levels (see Fig. S4 in the supplemental material) and nuclear Hdm2 levels (data not shown) upon LMB treatment. This result suggests that the Hdmx S367A mutant protein can enter the nucleus, like the corresponding wild-type protein, but cannot be retained in the nucleus following DNA damage. Previously, it was shown that overexpression of Hdm2 recruits Hdmx into

the nucleus (38). It should be noted that coexpression of ectopic Hdm2 resulted in increased nuclear localization of both the wild type and all Hdmx phosphorylation site mutant proteins (data not shown). Since treatment with LMB results in higher levels of Hdm2, the nuclear accumulation of Hdmx following this treatment could be Hdm2 dependent. To test this, we followed the LMB-induced nuclear accumulation of Hdmx in wild-type versus p53/Mdm2 double-knockout MEFs. Both wild-type Hdmx and the S367A mutant accumulate in the nucleus upon LMB treatment in wild-type MEFs. Importantly, a nuclear accumulation was also found in the p53/Mdm2 double-knockout MEFs, although the efficiency appears to be lower (Fig. 5C). These results suggest that LMB-induced nuclear accumulation of Hdmx is partly mediated by increased p53/Hdm2 levels but can also occur in a p53/Hdm2-independent and phosphorylation-independent manner. To further investigate whether high Hdm2 is sufficient for nuclear accumulation of Hdmx, we treated the transfected cells with nutlin-3, a potent and selective small-molecule antagonist of Hdm2 which had been shown to result in p53 stabilization and subsequent induction of Hdm2 levels (61). Since NCS treatment also activates p53, which results at later time points in increased Hdm2 levels, we compared the induction of Hdm2 levels following NCS, nutlin-3, or LMB treatment (see Fig. S5 in the supplemental material). LMB treatment of U2OS cells led to a slightly greater induction of Hdm2 than NCS treatment, but this slight difference could not explain the difference in effect regarding nuclear accumulation of Hdmx. Even more convincing, treatment of the transfected cells with nutlin-3 resulted in a strong increase in Hdm2 levels but no significant nuclear accumulation of Hdmx. All in all, these results suggest that increased Hdm2 expression upon DNA damage is not sufficient to lead to nuclear accumulation of Hdmx but that DSB-induced nuclear accumulation requires phosphorylation of Hdmx and interaction with other factors, such as 14-3-3 proteins. If, indeed, 14-3-3 proteins are involved in nuclear retention of phosphorylated Hdmx, it is possible that some nuclear accumulation of 14-3-3 occurs after DNA damage. To investigate this possibility, we examined the localization of both endogenous and exogenously expressed 14-3-3 tau protein. Both mock-transfected and HA-14-3-3-transfected cells were stained with the anti-14-3-3 tau monoclonal antibody. While 14-3-3 proteins localized mainly in the cytoplasm in untreated cells, following NCS treatment most cells also exhibited nuclear staining of endogenous and exogenously expressed 14-3-3 tau (see Fig. S6 in the supplemental material). It should be noted that the alteration in subcellular localization

---

(B) Competing 14-3-3 from Hdmx prevents DNA damage-induced nuclear accumulation of Hdmx. U2-OS cells were transfected with HA-Hdmx as described for panel A, but now in the presence of either YFP, YFP-difopein, or YFP-R18(Lys). Cells were stained with anti-Hdmx monoclonal antibody (6B1A). (C) LMB-induced Hdmx nuclear accumulation can occur independently of p53/Mdm2. Wild-type or p53$^{-/-}$ Mdm2$^{-/-}$ DKO MEFs were seeded in 6-cm dishes with coverslips. Cells were transfected with 1 μg of HA-Hdmx expression vectors. Twenty-four hours later, cells were either mock treated or treated with 10 nM leptomycin B for 8 h. Cells were stained with anti-Hdmx (6B1A) and with anti-p53 (FL393), and nuclei were counterstained with DAPI. Pictures were taken with a magnification-×63 lens. (D) Specificity of the anti-phospho-S367 antibody. MCF-7 cells were transfected with 150 ng of HA-Hdmx and 24 h later pretreated with 20 μM of MG132 for 30 min and subsequently with 500 ng/ml of NCS for 3 h. Cells were immunostained with the anti-phospho-S367 antibody (red) and anti-HA (green) in order to visualize total Hdmx. (E) Effect of Chk2 and ATM knockdown on S367 nuclear phosphorylation. A similar analysis as that for Fig. 5D was carried out with cells expressing shRNAs targeting Chk2, ATM, or GFP mRNA. Cells were pretreated with 20 μM of MG132 for 30 min, followed by 100 ng/ml of NCS for 3 h. Bar = 10 μm.

was not as striking as that seen with Hdmx, at least under these conditions. A significant cytoplasmic staining of 14-3-3 tau was always observed after NCS treatment. In the cotransfection experiment, 14-3-3 tau and Hdmx colocalized in both mock-treated and NCS-treated cells. These data indicate that 14-3-3 tau proteins are accumulating in the nucleus upon DNA damage, which can explain the importance of 14-3-3–Hdmx interaction for the nuclear accumulation of Hdmx. The results mentioned above would predict that S367-phosphorylated Hdmx protein would be strictly nuclear. We monitored the subcellular localization of S367 phosphorylation by immunostaining with the anti-pS367 antibody. To prevent the rapid degradation of phosphorylated Hdmx, the cells were pretreated with the proteasome inhibitor MG132. The anti-pS367 antibody also was found to be specific for S367-phosphorylated Hdmx in these experiments (Fig. 5D) and showed a strictly nuclear staining that is the same as total Hdmx staining, indicating that phosphorylation took place in the nucleus. In addition, DSB-induced accumulation of the S367-phosphorylated Hdmx was not detectable in cells knocked down for Chk2 or ATM expression (Fig. 5E). Furthermore, pretreatment of cells with the specific inhibitors for Chk2 and ATM also prevented the damage-induced nuclear accumulation of S367-phosphorylated Hdmx (see Fig. S7 in the supplemental material). These results suggest that Hdmx can enter the nucleus in the absence of DNA damage/phosphorylation on S367 but that nuclear Hdmx, which gets phosphorylated in an ATM- and Chk2-dependent manner following DNA damage, binds to nuclear 14-3-3 proteins and this complex is retained in the nucleus.

DISCUSSION

As the first transducer of the cellular response to DSBs, ATM typically approaches a downstream target from several directions. A prime example is ATM's control of the p53 pathway: in response to DSBs, ATM not only phosphorylates p53 directly but also orchestrates numerous other posttranslational modifications on p53 itself, as well as on its regulators, Hdm2 and Hdmx (35). ATM also activates other kinases (e.g., Chk1 and Chk2), which in turn phosphorylate their downstream effectors (24). In the case of Hdmx, both direct phosphorylation by ATM (12, 41, 45) and the indirect regulation via Chk2-mediated phosphorylation are needed to ensure a proper DNA damage-induced degradation of this protein. In this study we show that damage-induced phosphorylation of Hdmx by Chk2 leads to creation of binding sites for 14-3-3 proteins, nuclear accumulation, and proteasomal degradation. Respectively, Chk2-mediated phosphorylation was previously reported to mediate the degradation of the phosphatase Cdc25A in response to DNA damage, resulting in a rapid G_1/S checkpoint pathway (12). In addition, Chk2-mediated phosphorylation of the phosphatase Cdc25C also generates a landing pad for 14-3-3 proteins, leading to its sequestration from its substrates and maintenance of the G_2/M block (17, 32, 44, 67).

Binding of 14-3-3 proteins affects several players in the DNA damage responses. One of many ATM-mediated modifications along p53 is dephosphorylation of S376, which creates a binding site for 14-3-3 proteins at the nearby phospho-S378. Binding with 14-3-3 was shown to increase the affinity of p53 for specific DNA sequences (62). A mutant p53 protein, which

cannot interact with 14-3-3 proteins, still retained sequence-specific DNA binding, but its ability to activate the gene encoding p21^{WAF1} was compromised, as was its ability to induce a G_1 arrest (54). Given the role of Hdmx as an essential negative regulator of p53's transactivation activity (30), the important contribution of 14-3-3 proteins to the destabilization of Hdmx following DNA damage suggests that binding of these proteins is important in the activation of p53 as a transcription factor following DNA damage. A recent study indicated that in response to UV irradiation, 14-3-3γ and Chk1 are also essential regulators of Mdmx (20). These results combined indicate that 14-3-3 proteins contribute to p53's activation both directly by interacting with p53 and indirectly via control of Hdmx.

Another important player in the destabilization of Hdmx in response to DNA damage is the HAUSP ubiquitin protease (36). HAUSP's ability to deubiquitinate Hdmx and Hdm2 is reduced following DNA damage as a result of reduced affinity for these proteins. The dissociation of HAUSP from Hdmx was shown to be due to a caffeine-sensitive Hdmx phosphorylation event (36). Here we show that the inhibition of Hdmx-HAUSP interaction is dependent on Chk2. Since both 14-3-3–Hdmx and HAUSP-Hdmx interactions are Chk2 dependent, it is tempting to assume that 14-3-3 binding to Chk2-phosphorylated Hdmx directly competes with HAUSP binding. Alternatively, it can be assumed that binding of a 14-3-3 dimer to different sites on a target protein can strongly affect the structural organization. Possibly in this case the interaction of dimeric 14-3-3 with Hdmx changes the conformation of Hdmx in such a way that HAUSP cannot interact anymore, resulting in Hdmx destabilization following DNA damage. Another interesting possibility was raised by a recent report that identified P/AXXS as a consensus binding motif in HAUSP-interacting sequences in p53 and Mdm2 and determined the structural basis of their recognition (48). The authors identified six P/AXXS motifs on Hdmx: one of them, A^{398}HSS^{401}, is identical to one of the HAUSP binding sites on p53, and, like the p53 site, is close to a second potential HAUSP binding site with a PXXS motif. Furthermore, HAUSP binding motifs harboring a serine at position 3 may be subject to regulation of this interaction by phosphorylation, since a phosphoserine at this position is expected to prevent interaction with Glu162 of HAUSP (48). Interestingly, we recently identified ATM-mediated phosphorylation of S403 on Hdmx (45), which is located three positions upstream to such motif. Whether S403 phosphorylation is involved in the dissociation of HAUSP from Hdmx following DNA damage remains to be determined.

In summary, our data support a model (Fig. 6) in which efficient damage-induced degradation of Hdmx requires this protein to enter the nucleus, where it is phosphorylated by ATM and Chk2. These phosphorylations lead to the binding of Hdmx with several isoforms of the 14-3-3 proteins, subsequent retention of Hdmx in the nucleus, and dissociation from HAUSP, finally in the end leading to its degradation. Notably, DNA damage-induced Hdm2 destabilization was also shown recently to require the activity of the phosphatidylinositol 3-kinase kinases, most likely through Hdm2 phosphorylation at multiple sites. It was also suggested that such degradation occurs in the nucleus, since Hdm2 is largely nuclear and proteasome inhibition increases its nuclear abundance (56). Given that Hdm2 also serves as the
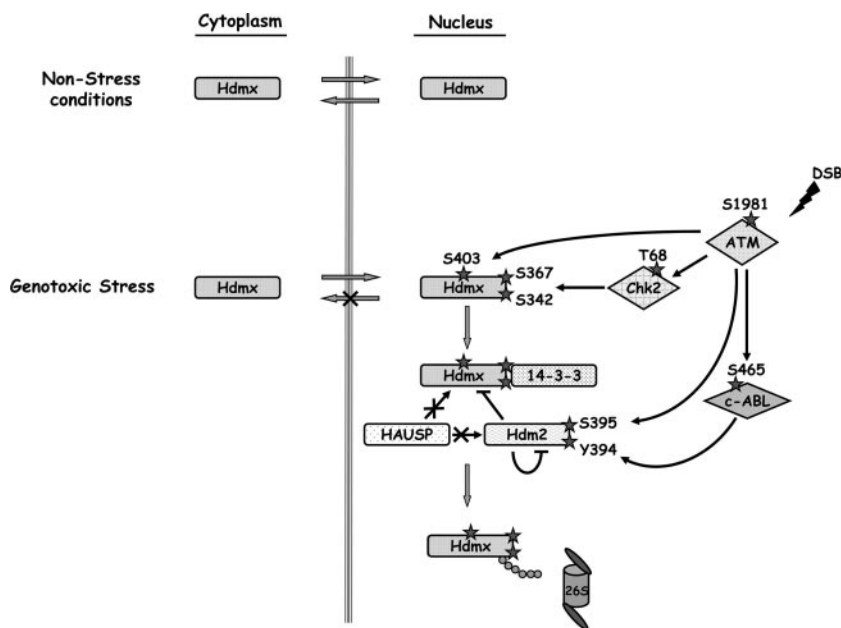
FIG. 6. Hdmx nuclear accumulation and degradation in response to DNA damage. In nonstressed cells, Hdmx can be found both in the cytoplasm and in the nucleus. In most cell lines, Hdmx is predominantly cytoplasmic. Following DSB induction, nuclear Hdmx is phosphorylated by ATM and Chk2. These phosphorylations result in binding of several 14-3-3 isoforms, which leads to nuclear retention of Hdmx and, subsequently, to its nuclear accumulation. Nuclear retention appears to be an essential step towards efficient Hdmx degradation.

E3 ubiquitin ligase that mediates the ubiquitination and degradation of Hdmx in response to DNA damage (21, 43), it is conceivable that an efficient degradation of Hdmx would require its recruitment to the nucleus.

The tight regulation of Hdmx by ATM and Chk2 following DSBs underscores the central role of this protein as an essential negative regulator of p53. Chk2 and ATM cooperate to achieve maximal p53-dependent expression of genes that are involved in sustained cell cycle arrest, certain forms of DNA repair, or promotion of apoptosis (4). The importance of Hdmx as a negative regulator of p53 gains support from the observation that degradation of Hdmx after DNA damage is essential for a proper p53 response, as evidenced by p53 stabilization, p21 induction, and activation of cell cycle checkpoints (21). While this paper was in preparation, another report confirmed that Chk2 and 14-3-3 cooperatively stimulate Mdmx ubiquitination and overcome the inhibition of p53 by Mdmx (25). Furthermore, three recent reports showed that Mdm2 and Mdmx are nonredundantly essential for preventing p53 activity. Although Mdm2 prevents accumulation of the p53 protein, Mdmx contributes to the overall inhibition of p53 activity independently of Mdm2. These reports proposed a model in which Mdm2 serves to mainly regulate p53 stability and Mdmx functions as a major inhibitor of p53 transcriptional activity (16, 29, 58, 64). Interestingly, a link between proliferation and S367 phosphorylation had already been made by Okamoto et al., who showed that S367A mutation enhanced the ability of Mdmx to suppress p53 and increased the growth of normal cells in culture (41).

Understanding the tight regulation of p53's negative regulator, Hdmx, mediated by Chk2 and ATM phosphorylations, might help unravel the complexity of the p53 axis of the DNA damage response. Furthermore, the results might point to ways to manipulate this inhibitor in cancer cells in which p53 inactivation occurs as a result of overexpressed Hdmx.

REFERENCES

1. **Ahn, J., M. Urist, and C. Prives.** 2004. The Chk2 protein kinase. DNA Repair (Amsterdam) **3:**1039–1047.
2. **Arienti, K. L., A. Brunmark, F. U. Axe, K. McClure, A. Lee, J. Blevitt, D. K. Neff, L. Huang, S. Crawford, C. R. Pandit, L. Karlsson, and J. G. Breitenbucher.** 2005. Checkpoint kinase inhibitors: SAR and radioprotective properties of a series of 2-arylbenzimidazoles. J. Med. Chem. **48:**1873–1885.
3. **Banin, S., L. Moyal, S. Shieh, Y. Taya, C. W. Anderson, L. Chessa, N. I. Smorodinsky, C. Prives, Y. Reiss, Y. Shiloh, and Y. Ziv.** 1998. Enhanced phosphorylation of p53 by ATM in response to DNA damage. Science **281:**1674–1677.
4. **Bartek, J., J. Falck, and J. Lukas.** 2001. CHK2 kinase—a busy messenger. Nat. Rev. Mol. Cell Biol. **2:**877–886.
5. **Bassing, C. H., and F. W. Alt.** 2004. The cellular response to general and programmed DNA double strand breaks. DNA Repair (Amsterdam) **3:**781–796.
6. **Biton, S., I. Dar, L. Mittelman, Y. Pereg, A. Barzilai, and Y. Shiloh.** 2006. Nuclear ataxia-telangiectasia mutated (ATM) mediates the cellular response to DNA double strand breaks in human neuron-like cells. J. Biol. Chem. **281:**17482–17491.
7. **Böttger, V., A. Böttger, C. Garcia-Echeverria, Y. F. Ramos, A. J. van der Eb,**

A. G. Jochemsen, and D. P. Lane. 1999. Comparative study of the p53-mdm2 and p53-MDMX interfaces. Oncogene 18:189–199.

8. Brown, K. D., Y. Ziv, S. N. Sadanandan, L. Chessa, F. S. Collins, Y. Shiloh, and D. A. Tagle. 1997. The ataxia-telangiectasia gene product, a constitutively expressed nuclear protein that is not up-regulated following genome damage. Proc. Natl. Acad. Sci. USA 94:1840–1845.

9. Brummelkamp, T. R., R. Bernards, and R. Agami. 2002. A system for stable expression of short interfering RNAs in mammalian cells. Science 296:550–553.

10. Cahill, C. M., G. Tzivion, N. Nasrin, S. Ogg, J. Dore, G. Ruvkun, and M. Alexander-Bridges. 2001. Phosphatidylinositol 3-kinase signaling inhibits DAF-16 DNA binding and function via 14-3-3-dependent and 14-3-3-independent pathways. J. Biol. Chem. 276:13402–13410.

11. Chen, J., V. Marechal, and A. J. Levine. 1993. Mapping of the p53 and mdm-2 interaction domains. Mol. Cell. Biol. 13:4107–4114.

12. Chen, L., D. M. Gilkes, Y. Pan, W. S. Lane, and J. Chen. 2005. ATM and Chk2-dependent phosphorylation of MDMX contribute to p53 activation after DNA damage. EMBO J. 24:3411–3422.

13. Clokie, S. J., K. Y. Cheung, S. Mackie, R. Marquez, A. H. Peden, and A. Aitken. 2005. BCR kinase phosphorylates 14-3-3 Tau on residue 233. FEBS J. 272:3767–3776.

14. de Graaf, P., N. A. Little, Y. F. Ramos, E. Meulmeester, S. J. Letteboer, and A. G. Jochemsen. 2003. Hdmx protein stability is regulated by the ubiquitin ligase activity of Mdm2. J. Biol. Chem. 278:38315–38324.

15. Dunaway, S., H. Y. Liu, and N. C. Walworth. 2005. Interaction of 14-3-3 protein with Chk1 affects localization and checkpoint function. J. Cell Sci. 118:39–50.

16. Francoz, S., P. Froment, S. Bogaerts, S. De Clercq, M. Maetens, G. Doumont, E. Bellefroid, and J. C. Marine. 2006. Mdm4 and Mdm2 cooperate to inhibit p53 activity in proliferating and quiescent cells in vivo. Proc. Natl. Acad. Sci. USA 103:3232–3237.

17. Graves, P. R., C. M. Lovly, G. L. Uy, and H. Piwnica-Worms. 2001. Localization of human Cdc25C is regulated both by nuclear export and 14-3-3 protein binding. Oncogene 20:1839–1851.

18. Harris, S. L., and A. J. Levine. 2005. The p53 pathway: positive and negative feedback loops. Oncogene 24:2899–2908.

19. Hickson, I., Y. Zhao, C. J. Richardson, S. J. Green, N. M. Martin, A. I. Orr, P. M. Reaper, S. P. Jackson, N. J. Curtin, and G. C. Smith. 2004. Identification and characterization of a novel and specific inhibitor of the ataxia-telangiectasia mutated kinase ATM. Cancer Res. 64:9152–9159.

20. Jin, Y., M. S. Dai, S. Z. Lu, Y. Xu, Z. Luo, Y. Zhao, and H. Lu. 2006. 14-3-3γ binds to MDMX that is phosphorylated by UV-activated Chk1, resulting in p53 activation. EMBO J. 25:1207–1218.

21. Kawai, H., D. Wiederschain, H. Kitao, J. Stuart, K. K. Tsai, and Z. M. Yuan. 2003. DNA damage-induced MDMX degradation is mediated by MDM2. J. Biol. Chem. 278:45946–45953.

22. Khosravi, R., R. Maya, T. Gottlieb, M. Oren, Y. Shiloh, and D. Shkedy. 1999. Rapid ATM-dependent phosphorylation of MDM2 precedes p53 accumulation in response to DNA damage. Proc. Natl. Acad. Sci. USA 96:14973–14977.

23. Kim, S. T., B. Xu, and M. B. Kastan. 2002. Involvement of the cohesin protein, Smc1, in Atm-dependent and independent responses to DNA damage. Genes Dev. 16:560–570.

24. Kurz, E. U., and S. P. Lees-Miller. 2004. DNA damage-induced activation of ATM and ATM-dependent signaling pathways. DNA Repair (Amsterdam) 3:889–900.

25. Lebron, C., L. Chen, D. M. Gilkes, and J. Chen. 2006. Regulation of MDMX nuclear import and degradation by Chk2 and 14-3-3. EMBO J. 25:1196–1206.

26. Li, C., L. Chen, and J. Chen. 2002. DNA damage induces MDMX nuclear translocation by p53-dependent and -independent mechanisms. Mol. Cell. Biol. 22:7562–7571.

27. Lukas, J., C. Lukas, and J. Bartek. 2004. Mammalian cell cycle checkpoints: signalling pathways and their organization in space and time. DNA Repair (Amsterdam) 3:997–1007.

28. Mackintosh, C. 2004. Dynamic interactions between 14-3-3 proteins and phosphoproteins regulate diverse cellular processes. Biochem. J. 381:329–342.

29. Marine, J. C., S. Francoz, M. Maetens, G. Wahl, F. Toledo, and G. Lozano. 2006. Keeping p53 in check: essential and synergistic functions of Mdm2 and Mdm4. Cell Death Differ. 13:927–934.

30. Marine, J. C., and A. G. Jochemsen. 2004. Mdmx and Mdm2: brothers in arms? Cell Cycle 3:900–904.

31. Masters, S. C., and H. Fu. 2001. 14-3-3 proteins mediate an essential anti-apoptotic signal. J. Biol. Chem. 276:45193–45200.

32. Matsuoka, S., M. Huang, and S. J. Elledge. 1998. Linkage of ATM to cell cycle regulation by the Chk2 protein kinase. Science 282:1893–1897.

33. Matsuoka, S., G. Rotman, A. Ogawa, Y. Shiloh, K. Tamai, and S. J. Elledge. 2000. Ataxia telangiectasia-mutated phosphorylates Chk2 in vivo and in vitro. Proc. Natl. Acad. Sci. USA 97:10389–10394.

34. Maya, R., M. Balass, S. T. Kim, D. Shkedy, J. F. Leal, O. Shifman, M. Moas, T. Buchmann, Z. Ronai, Y. Shiloh, M. B. Kastan, E. Katzir, and M. Oren. 2001. ATM-dependent phosphorylation of Mdm2 on serine 395: role in p53 activation by DNA damage. Genes Dev. 15:1067–1077.

35. Meek, D. W. 2004. The p53 response to DNA damage. DNA Repair (Amsterdam) 3:1049–1056.

36. Meulmeester, E., M. M. Maurice, C. Boutell, A. F. Teunisse, H. Ovaa, T. E. Abraham, R. W. Dirks, and A. G. Jochemsen. 2005. Loss of HAUSP-mediated deubiquitination contributes to DNA damage-induced destabilization of Hdmx and Hdm2. Mol. Cell 18:565–576.

37. Michael, D., and M. Oren. 2002. The p53 and Mdm2 families in cancer. Curr. Opin. Genet. Dev. 12:53–59.

38. Migliorini, D., E. Lazzerini Denchi, D. Danovi, A. Jochemsen, M. Capillo, A. Gobbi, K. Helin, P. G. Pelicci, and J. C. Marine. 2002. Mdm4 (Mdmx) regulates p53-induced growth arrest and neuronal cell death during early embryonic mouse development. Mol. Cell. Biol. 22:5527–5538.

39. Moll, U. M., and O. Petrenko. 2003. The MDM2-p53 interaction. Mol. Cancer Res. 1:1001–1008.

40. Muslin, A. J., J. W. Tanner, P. M. Allen, and A. S. Shaw. 1996. Interaction of 14-3-3 with signaling proteins is mediated by the recognition of phosphoserine. Cell 84:889–897.

41. Okamoto, K., K. Kashima, Y. Pereg, A. Ishida, S. Yamazaki, A. Nota, A. Teunisse, D. Migliorini, I. Kitabayashi, J. C. Marine, C. Prives, Y. Shiloh, A. G. Jochemsen, and Y. Taya. 2005. DNA damage-induced phosphorylation of MdmX at serine 367 activates p53 by targeting MdmX for Mdm2-dependent degradation. Mol. Cell. Biol. 25:9608–9620.

42. Oren, M. 2003. Decision making by p53: life, death and cancer. Cell Death Differ. 10:431–442.

43. Pan, Y., and J. Chen. 2003. MDM2 promotes ubiquitination and degradation of MDMX. Mol. Cell. Biol. 23:5113–5121.

44. Peng, C. Y., P. R. Graves, R. S. Thoma, Z. Wu, A. S. Shaw, and H. Piwnica-Worms. 1997. Mitotic and G2 checkpoint control: regulation of 14-3-3 protein binding by phosphorylation of Cdc25C on serine-216. Science 277:1501–1505.

45. Pereg, Y., D. Shkedy, P. de Graaf, E. Meulmeester, M. Edelson-Averbukh, M. Salek, S. Biton, A. F. Teunisse, W. D. Lehmann, A. G. Jochemsen, and Y. Shiloh. 2005. Phosphorylation of Hdmx mediates its Hdm2- and ATM-dependent degradation in response to DNA damage. Proc. Natl. Acad. Sci. USA 102:5056–5061.

46. Seimiya, H., H. Sawada, Y. Muramatsu, M. Shimizu, K. Ohko, K. Yamane, and T. Tsuruo. 2000. Involvement of 14-3-3 proteins in nuclear localization of telomerase. EMBO J. 19:2652–2661.

47. Shen, Y. H., J. Godlewski, A. Bronisz, J. Zhu, M. J. Comb, J. Avruch, and G. Tzivion. 2003. Significance of 14-3-3 self-dimerization for phosphorylation-dependent target binding. Mol. Biol. Cell 14:4721–4733.

48. Sheng, Y., V. Saridakis, F. Sarkari, S. Duan, T. Wu, C. H. Arrowsmith, and L. Frappier. 2006. Molecular recognition of p53 and MDM2 by USP7/HAUSP. Nat. Struct. Mol. Biol. 13:285–291.

49. Shiloh, Y. 2003. ATM and related protein kinases: safeguarding genome integrity. Nat. Rev. Cancer 3:155–168.

50. Shvarts, A., W. T. Steegenga, N. Riteco, T. van Laar, P. Dekker, M. Bazuine, R. C. van Ham, W. van der Houven van Oordt, G. Hateboer, A. J. van der Eb, and A. G. Jochemsen. 1996. MDMX: a novel p53-binding protein with some functional properties of MDM2. EMBO J. 15:5349–5357.

51. Slee, E. A., D. J. O'Connor, and X. Lu. 2004. To die or not to die: how does p53 decide? Oncogene 23:2809–2818.

52. Stad, R., N. A. Little, D. P. Xirodimas, R. Frenk, A. J. van der Eb, D. P. Lane, M. K. Saville, and A. G. Jochemsen. 2001. Mdmx stabilizes p53 and Mdm2 via two distinct mechanisms. EMBO Rep. 2:1029–1034.

53. Stad, R., Y. F. Ramos, N. Little, S. Grivell, J. Attema, A. J. van der Eb, and A. G. Jochemsen. 2000. Hdmx stabilizes Mdm2 and p53. J. Biol. Chem. 275:28039–28044.

54. Stavridi, E. S., N. H. Chehab, A. Malikzay, and T. D. Halazonetis. 2001. Substitutions that compromise the ionizing radiation-induced association of p53 with 14-3-3 proteins also compromise the ability of p53 to induce cell cycle arrest. Cancer Res. 61:7030–7033.

55. Stevens, C., L. Smith, and N. B. La Thangue. 2003. Chk2 activates E2F-1 in response to DNA damage. Nat. Cell Biol. 5:401–409.

56. Stommel, J. M., and G. M. Wahl. 2004. Accelerated MDM2 auto-degradation induced by DNA-damage kinases is required for p53 activation. EMBO J. 23:1547–1556.

57. Tanimura, S., S. Ohtsuka, K. Mitsui, K. Shirouzu, A. Yoshimura, and M. Ohtsubo. 1999. MDM2 interacts with MDMX through their RING finger domains. FEBS Lett. 447:5–9.

58. Toledo, F., K. A. Krummel, C. J. Lee, C. W. Liu, L. W. Rodewald, M. Tang, and G. M. Wahl. 2006. A mouse p53 mutant lacking the proline-rich domain rescues Mdm4 deficiency and provides insight into the Mdm2-Mdm4-p53 regulatory network. Cancer Cell 9:273–285.

59. Tzivion, G., Z. Luo, and J. Avruch. 1998. A dimeric 14-3-3 protein is an essential cofactor for Raf kinase activity. Nature 394:88–92.

60. Tzivion, G., Y. H. Shen, and J. Zhu. 2001. 14-3-3 proteins; bringing new definitions to scaffolding. Oncogene 20:6331–6338.

61. Vassilev, L. T., B. T. Vu, B. Graves, D. Carvajal, F. Podlaski, Z. Filipovic, N.Kong, U. Kammlott, C. Lukacs, C. Klein, N. Fotouhi, and E. A. Liu. 2004. In vivo activation of the p53 pathway by small-molecule antagonists of MDM2. Science 303:844–848.

62. Waterman, M. J., E. S. Stavridi, J. L. Waterman, and T. D. Halazonetis.

1998. ATM-dependent activation of p53 involves dephosphorylation and association with 14-3-3 proteins. Nat. Genet. **19:**175–178.

63. **Wilker, E., and M. B. Yaffe.** 2004. 14-3-3 proteins–a focus on cancer and human disease. J. Mol. Cell Cardiol. **37:**633–642.

64. **Xiong, S., C. S. Van Pelt, A. C. Elizondo-Fraire, G. Liu, and G. Lozano.** 2006. Synergistic roles of Mdm2 and Mdm4 for p53 inhibition in central nervous system development. Proc. Natl. Acad. Sci. USA **103:**3226–3231.

65. **Yazdi, P. T., Y. Wang, S. Zhao, N. Patel, E. Y. Lee, and J. Qin.** 2002. SMC1 is a downstream effector in the ATM/NBS1 branch of the human S-phase checkpoint. Genes Dev. **16:**571–582.

66. **Zannini, L., D. Lecis, S. Lisanti, R. Benetti, G. Buscemi, C. Schneider, and D. Delia.** 2003. Karyopherin-alpha2 protein interacts with Chk2 and contributes to its nuclear import. J. Biol. Chem. **278:**42346–42351.

67. **Zeng, Y., and H. Piwnica-Worms.** 1999. DNA damage and replication checkpoints in fission yeast require nuclear exclusion of the Cdc25 phosphatase via 14-3-3 binding. Mol. Cell. Biol. **19:**7410–7419.